

Design of a Reconfigurable Exoskeleton used on Human Locomotion Recovery

Dumitru N., Copilusi C., Dumitru S. and Rosu E

Abstract—This paper describes a reconfigurable leg exoskeleton designed for human locomotion system rehabilitation. The designed exoskeleton consists of two equivalent lower limbs, a special frame and a command and control unit. The research core was focused on the actuation mechanism, which this can be replaced by physician specific requirements. Thus, there were proposed two types of actuation systems, namely linear electric motors and cam mechanisms with rotational electric motors. The starting actuation system solution was represented by the linear electric motors and this needs to be improved. For this, a human gait experimental analysis was performed in order to obtain the input data for cam mechanism designs. Based on this, a mathematical model of the cam actuation mechanism was developed from where the cam profiles were obtained. The cam mechanism fits perfectly the human locomotion system especially for knee and ankle joints. Thus it will be elaborated and numerically processed mathematical models for cam mechanism design respectively linear motion laws identification for linear actuators. The obtained results, starting from theoretical analyses to a prototype, validate both actuation systems and certify the reconfigurable solution.

Keywords—cam mechanism, exoskeleton design, human locomotion, reconfigurable mechatronic system.

I. INTRODUCTION

TODAY human exoskeletons design is in a continuous growth. These are used in several domains like army, industry, medicine and even space exploration. By considering the ones used in medicine, several exoskeleton types were designed especially for human walking rehabilitation. From this category, it can be observed the ones from [1] – [8] especially designed for persons with neuromotor disorders or stroke accidents. Other exoskeletons like [9] – [15] were designed for human walking temporal recovery programs in case of persons which have to follow specific locomotion recovery therapies after surgical interventions. By considering this research area, it can be identified many design conditions, namely: actuation complexity, low-cost principles, comfort

conditions, user-friendly interface, easy-operation features. By considering these design conditions, some of the existent exoskeleton like [5] and [6] accomplish a part of these, others like [9] [10] fulfill all, but they are complex ones and leads to expensive rehabilitation programs. Also these require a special rehabilitation team consists on a proper physician, a medical engineer, a technician and a couple of rehabilitation assistants.

Another argument is imposed by the physician specific requirements, which are different in most medical cases especially for persons who need human walking assistance during recovery and rehabilitation programs. For these cases, human exoskeletons are characterized by complex actuation mechanisms with a minimum number of actuators [3], [6], [12] and [16], others were designed based on a simplified structure with a large number of actuators and a complex command&control system like [8], [15] and [17].

In order to have in our sight the physician needs, as input data, a reconfigurable leg exoskeleton concept was designed, in order to serve in two modes: one mode for rehabilitation programs (designed for stroke accidents and some neuromotor disorders); other mode for temporal recovery programs (after minor injuries or superficial surgical interventions). By taking into account these actuation solutions as a starting point, it was needed a human walking experimental analysis for creating a database characterized by hip, knee and ankle joints motion laws and trajectories. The procedure for achieving this database is described in second section of the paper and it offers essential data for designing the reconfigurable leg exoskeleton for both actuation systems types. Meanwhile, there were analyzed several exoskeleton types from mechanical viewpoints and in third section are presented two actuation mechanisms which can be placed on the same exoskeleton leg mechanical structure. In this way the designed leg exoskeleton will have a reconfigurable structure and is described in third section. The exoskeleton design starts from an existent solution namely the one with linear electric actuators, which this can be improved for running in a continuous mode due to the physician requirements. In this way two cam actuation mechanisms were especially designed from theoretical viewpoints to a prototype model, namely one for knee joint and other for ankle joint motions. The created mathematical model obtained through this research leads to cam profile analysis based on kinematical approaches. For motion laws identification of the drive joints an inverse kinematic analysis will be performed for cam mechanism solution, by using as input data the proposed human

This work was supported by a grant of the Romanian National Authority for Scientific Research and Innovation, PN-III-P2-2.1-PED-2016-0934.

N. Dumitru is with the Faculty of Mechanics, University of Craiova. Calea Bucuresti no. 107. Romania (e-mail: nicolae_dtru@yahoo.com)

C. Copilusi is with the Faculty of Mechanics, University of Craiova. Calea Bucuresti no. 107. Romania (corresponding author to provide phone: +04 0747222771; e-mail: cristache03@yahoo.co.uk).

S. Dumitru, is with the Faculty of Automation, Computers and Electronics, University of Craiova. Bulevardul Decebal no. 107. Romania (e-mail: dumitrusorin83@yahoo.com).

E. Rosu is with the Faculty of Mechanics, University of Craiova. Calea Bucuresti no. 107. Romania (e-mail: acasa@mectrat.ro).

experimental analysis. By elaborating a virtual model, this can be analyzed based on kinematic and dynamic imposed conditions with MSC Adams software and this is presented on fourth section where also it is analyzed through experimental tests. At the end several major conclusions were obtained which characterize the reconfigurable leg exoskeleton validation.

II. EXPERIMENTAL ANALYSIS OF HUMAN WALKING

The human walking experimental analysis was performed with the aid of a CONTEMPLAS Equipment [18]. This equipment use a workflow summary described in Fig. 1 and it has 2 high-speed cameras which can record motions with a speed of 350 frames/second.

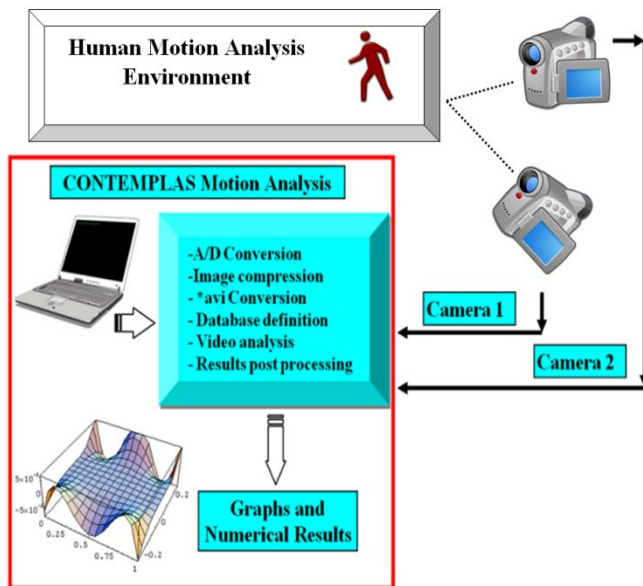


Fig. 1 Experimental analysis workflow by using CONTEMPLAS Equipment

The analysis principle requires the attachment of a reflexive markers on each desired joint from the analyzed human subject structure as it can be remarked on Fig. 2. The TEMPLO Motion software will recognize in real time the position, velocities and accelerations of this, when the analyzed human subject will perform motions. The obtained results can be useful as input data for further mathematical models elaborations and also on virtual simulations with specific software packages for validating the desired models. In this way a database was created which consists of 10 human subjects (5 male and 5 female persons) used on walking activity recordings. The chosen human subjects have various anthropometric data as it follows: age between 21 and 35 years old, weight between 48 and 102 kilograms, height between 1.5 meters and 1.85 meters, foot length between 305 millimeters and 497 millimeters. Some snapshots during recordings are shown in Fig. 3.

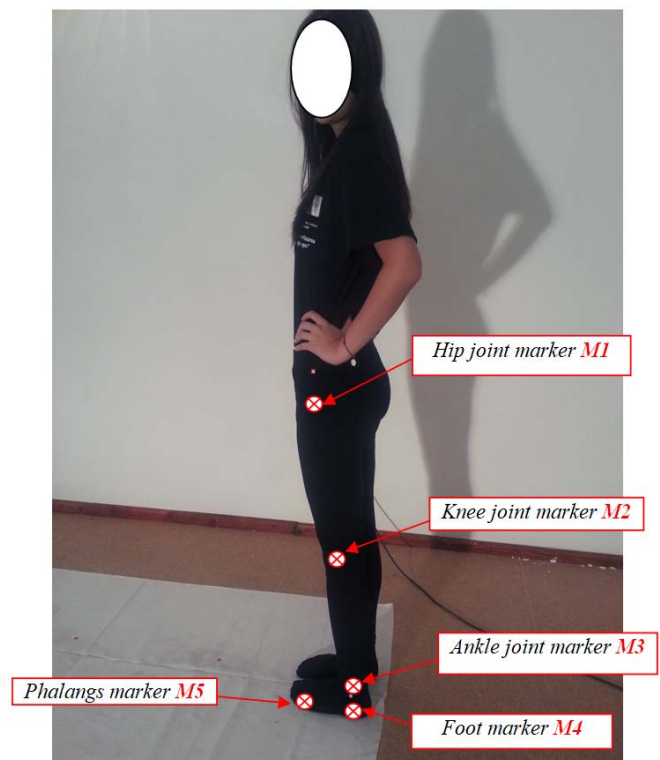


Fig. 2 Marker attachment on an analyzed human subject

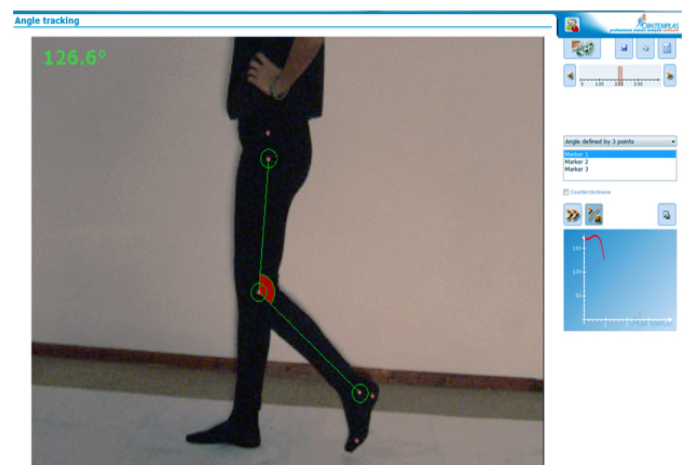


Fig. 3 Snapshot during experimental analysis

The desired motion laws for this analysis were validated only for a single gait, in case of hips, knees and ankles during walking activity. The captured gait varies between 1.2 seconds to 2.4 seconds. The desired data can be exported in a *.txt extension format that can be operated with various data management programs.

Through the obtained database it was identified the analyzed joints angular variations limit and these are shown in Fig. 4, Fig. 5 and Fig. 6.

Considering the obtained graphs from Fig. 4, Fig. 5 and Fig. 6, it can be identified the gait phases and the proper values for writing the specific code protocols of the command&control unit in case of the leg exoskeleton actuated with linear actuators.

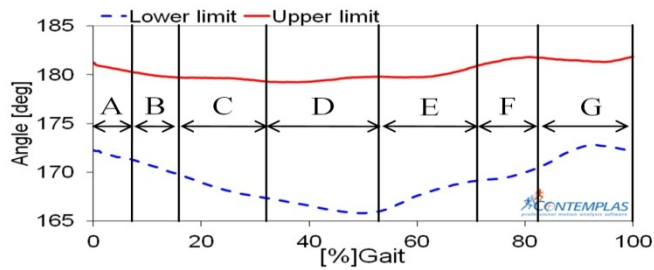


Fig. 4 Measured limits of the hip joint angle as a function of % for a complete gait

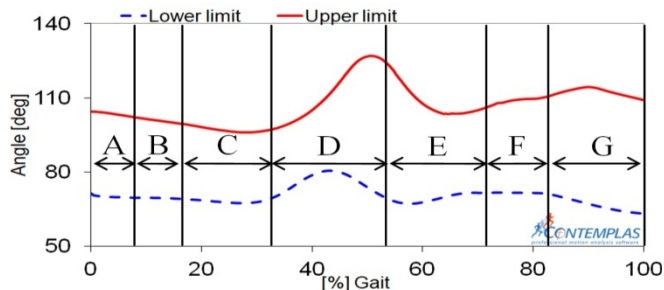


Fig. 5 Measured limits of the knee joint angle as a function of % for a complete gait

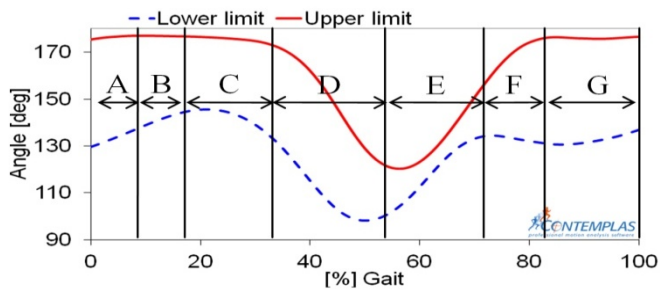


Fig. 6 Measured limits of the ankle joint angle as a function of % for a complete gait

Thus, the following correspondence was obtained: A-zone for heel strike; B, C – zone for loading response and mid-stance; D- zone for terminal stance; E- zone for pre-swing; F – zone for toe-off; G – zone for mid-swing and terminal swing.

These results were validated after a comparative study with similar ones from literature as in [19] and in Fig. 7 these phases are presented in a schematic form [20].

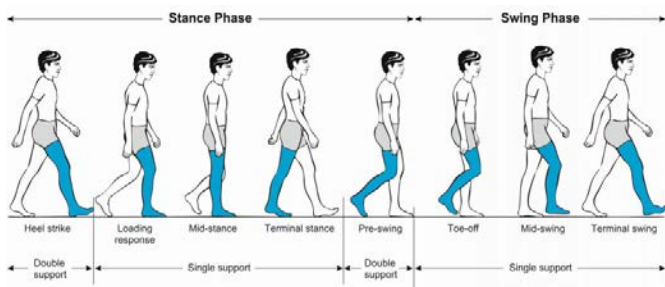


Fig. 7 Gait phases during human walking [20]

This remark should be addressed due to the further research stages, where time was a variable and should be expressed in a numerical form.

III. RECONFIGURABLE LEG EXOSKELETON DESIGN

By taking into account the research objective, there was considered a common leg exoskeleton linkage which will serve for two actuation systems, namely actuation through cam mechanisms and actuation through linear electric actuators. Thus, in Fig. 8 a first kinematic scheme of the linkage with cam mechanisms will be proposed.

This actuation solution was generated by a kinematic analysis of the human lower limb. This is a parameterized one due to the anthropometric data obtained on experimental analysis database. In Fig. 8, the following components will be identified: 1 – cam profile for knee joint actuation; 2 – cam follower support link; 3, 4, 5 – links for moving the knee linkage mechanism; 6 – link connected to the tibia equivalent segment (in point Q); 7 – cam profile for ankle joint actuation; 8 – cam follower support link for ankle joint actuation; 9, 10, 11 – links for moving the ankle linkage mechanism; 12 – link equivalent to the foot segment; A, B, C, D, E, F, G, H, I, K, M, N, P, O, R, S – revolute joints.

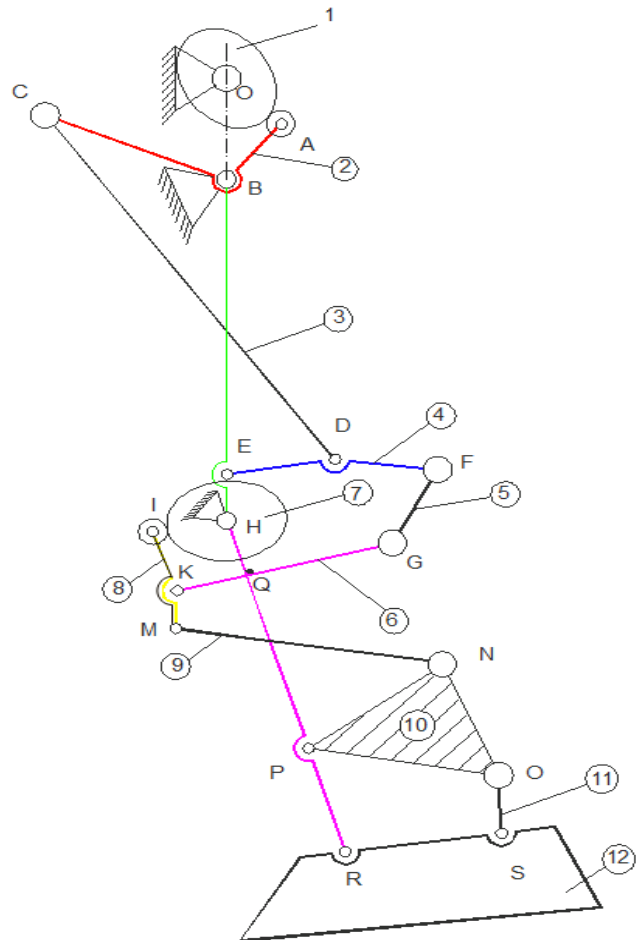


Fig. 8 Leg exoskeleton with cam mechanism actuation structural scheme

This mechanism linkage use only two rotational electric motors placed on O and H joints. Hip joint in this case will be actuated straight to the rotational motor placed on O joint.

The proposed exoskeleton mechanism was analyzed from kinematic and dynamic considerations in [8] and [9]. Some reports with appropriate theoretical studies can be found in [23] and [24]. Thus, the cam profiles were designed based on human motions developed during walking by hip, knee and ankle joints.

For generating the cam profiles a mechanism synthesis analysis was performed. The procedure was applied for both cam mechanisms, namely knee and ankle actuation ones. Thus, a summary analysis will be presented only for ankle actuation mechanism and a detailed analysis can be found in [3, 4]. For this, there were considered two design possibilities: one when the foot segment is not in contact with the ground and other when this is fully constrained. Thus, a model was defined in Cartesian coordinates as it can be seen in Fig. 9. The mathematical models numerical processing for the cam profile was based on the law knee and ankle joint angle variations. These laws have been obtained through an experimental synthesis of the analyzed human subjects as it can be remarked on Fig. 5 and Fig. 6.

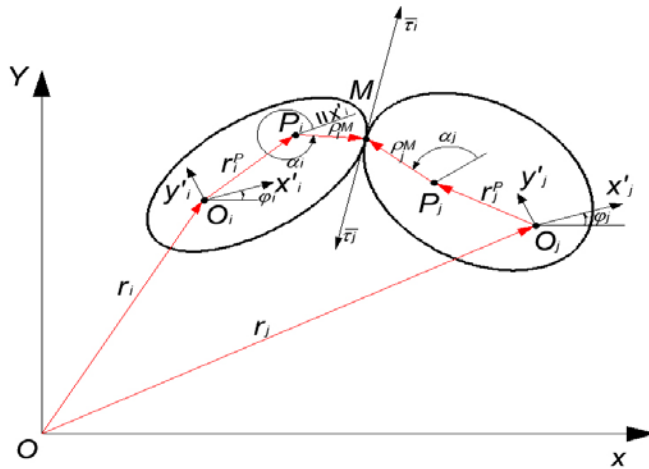


Fig. 9 Cam mechanism design based on common tangency condition

There are considered the following reference systems:

$T(X, Y)$ - the global reference system; T_i' (x_i', y_i') - the reference system joint with element i ; T_j' (x_j', y_j') - the reference system joint with element j ; (X_i, Y_i) , (X_j, Y_j) - the coordinates of points O_i' and O_j' in relation to the global reference system T .

The position vector for M contact point depending on T_i' reference system is represented by:

$$r_i'^M = r_i'^P + S_i'^M \quad (1)$$

$$S_i'^M = \delta_i(\alpha_i) \cdot v_i'(\alpha_i) \quad (2)$$

where: $\delta_i(\alpha_i)$ is the length of $S_i'^M$ curve radius with:

$$v_i'(\alpha_i) = [\cos \alpha_i \quad \sin \alpha_i]^T \quad (3)$$

The cam profile annotated with “ i ” will be obtained based on cubic spline interpolation with numerical data.

The tangent vector at “ i ”, respectively “ j ” in M contact point is:

$$\tau_i' = \frac{dS_i'^M}{d\alpha_i} = \frac{d\rho_i(\alpha_i)}{d\alpha_i} \cdot v_i'(\alpha_i) + \rho_i(\alpha_i) \frac{dv_i'(\alpha_i)}{d\alpha_i} \quad (4)$$

$$\tau_j' = \frac{dS_j'^M}{d\alpha_j} = \frac{d\rho_j(\alpha_j)}{d\alpha_j} \cdot v_j'(\alpha_j) + \rho_j(\alpha_j) \frac{dv_j'(\alpha_j)}{d\alpha_j} \quad (5)$$

The common tangency condition between cam element and cam follower can be expressed as:

$$(\tau_i^\perp)^T \tau_j = 0 \quad (6)$$

$$\begin{aligned} (\tau_i^\perp)^T &= (R \cdot \tau_i)^T = \tau_i^T \cdot R^T = \\ &= (A_{0i} \tau_i')^T R^T = \tau_i'^T \cdot A_{0i}^T \cdot R^T \end{aligned} \quad (7)$$

$$\tau_i'^T \cdot A_{0i}^T \cdot R^T \cdot A_{0j} \tau_j' = -\tau_i'^T \cdot A_{ij} \cdot \tau_j' = 0 \quad (8)$$

Where: τ_i^\perp - normal vector on τ_i ; R - rotation matrix, A_{0j} - is the coordinate transformation matrix for crossing from local coordinates system T_j' to global one, namely T ; $S_i'^M$ - is the position vector of M point depending on T_j' . The coordinate transformation matrix has the following form:

$$A_{0i} = \begin{bmatrix} \cos \varphi_i & -\sin \varphi_i \\ \sin \varphi_i & \cos \varphi_i \end{bmatrix} \quad (9)$$

$$A_{0j} = \begin{bmatrix} \cos \varphi_j & -\sin \varphi_j \\ \sin \varphi_j & \cos \varphi_j \end{bmatrix} \quad (10)$$

$$R = \begin{bmatrix} 0 & -1 \\ 1 & 0 \end{bmatrix} \quad (11)$$

The contact condition between cam element and cam follower in point M is:

$$r_i + r_i^P + S_i^M - S_j^M - r_j^P - r_j = 0 \quad (12)$$

$$\begin{bmatrix} x_i \\ y_i \end{bmatrix} + A_{0i} \cdot r_i^P + A_{0i} \cdot S_i^M - \\ - A_{0j} \cdot S_j^M - A_{0j} \cdot r_j^P - \begin{bmatrix} x_j \\ y_j \end{bmatrix} = 0 \quad (13)$$

$$\begin{bmatrix} x_i \\ y_i \end{bmatrix} + \begin{bmatrix} \cos \varphi_i & -\sin \varphi_i \\ \sin \varphi_i & \cos \varphi_i \end{bmatrix} \cdot \begin{bmatrix} x_i^P & S_i^{Mx} \\ y_i^P & S_i^{My} \end{bmatrix} - \begin{bmatrix} \cos \varphi_j & -\sin \varphi_j \\ \sin \varphi_j & \cos \varphi_j \end{bmatrix} \cdot \begin{bmatrix} S_j^{Mx} & -x_j^P \\ S_j^{My} & -y_j^P \end{bmatrix} - \begin{bmatrix} x_i \\ y_i \end{bmatrix} = 0 \quad (14)$$

$$r_j^M = r_j^P + S_j^M \quad (15)$$

$$x_j^M = r \cos \alpha_j \quad (16)$$

$$y_j^M = l_2 + r \sin \alpha_j \quad (17)$$

$$\alpha_j = -\varphi_j + \arctan \left(\frac{-\omega_j \cdot l_2 \cdot \sin \varphi_j + \omega_j (y_j - y_i)}{-\omega_j \cdot l_2 \cdot \cos \varphi_j + \omega_j (x_j - x_i)} \right) \quad (18)$$

Where: l_2 – cam follower length; α_j - represents the angle established from kinematic conditions, as it can be remarked in Fig. 10.

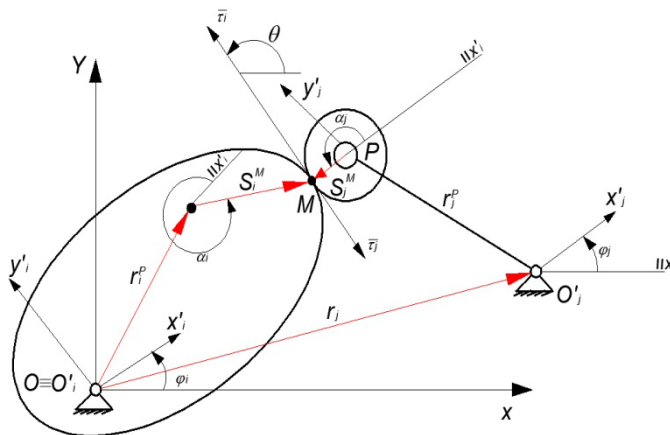


Fig. 10 Contact condition expressed in Cartesian coordinates

By taking into account the represented parameters from Fig. 10, the contact condition in Cartesian coordinates is represented by:

$$r_i + r_i^M = r_j + r_j^M \quad (19)$$

$$\begin{bmatrix} x_i \\ y_i \end{bmatrix} + \begin{bmatrix} \cos \varphi_i & -\sin \varphi_i \\ \sin \varphi_i & \cos \varphi_i \end{bmatrix} \cdot \begin{bmatrix} x_i^M \\ y_i^M \end{bmatrix} = \begin{bmatrix} x_j \\ y_j \end{bmatrix} + \begin{bmatrix} \cos \varphi_j & -\sin \varphi_j \\ \sin \varphi_j & \cos \varphi_j \end{bmatrix} \cdot \begin{bmatrix} x_j^M \\ y_j^M \end{bmatrix} \quad (20)$$

$$\begin{cases} x_i + \cos \varphi_i \cdot x_i^M - \sin \varphi_i \cdot y_i^M - x_j - \cos \varphi_j \cdot x_j^M + \sin \varphi_j \cdot y_j^M = 0 \\ y_i + \sin \varphi_i \cdot x_i^M + \cos \varphi_i \cdot y_i^M - y_j - \sin \varphi_j \cdot x_j^M - \cos \varphi_j \cdot y_j^M = 0 \end{cases} \quad (21)$$

$$x_j^M = r \cos \alpha_j \quad (22)$$

$$y_j^M = r \sin \alpha_j + l_2 \quad (23)$$

$$\begin{cases} x_i + \cos \varphi_i \cdot x_i^M - \sin \varphi_i \cdot y_i^M - a - \cos \varphi_j \cdot r \cdot \cos \alpha_j + \sin \varphi_j (l_2 + r \cdot \sin \alpha_j) = 0 \\ y_i + \sin \varphi_i \cdot x_i^M + \cos \varphi_i \cdot y_i^M - b - \sin \varphi_j \cdot r \cdot \cos \alpha_j - \cos \varphi_j (l_2 + r \cdot \sin \alpha_j) = 0 \end{cases} \quad (24)$$

$$\varphi_i = \omega_i \cdot t \quad (25)$$

Where: φ_i - cam element motion law; r – cam follower radius; φ_j – cam follower motion law, established through an inverse kinematic analysis [8].

Finally the kinematic constraints equations for cam mechanism design resulted from common tangency condition and contact conditions are obtained as it follows:

$$\begin{cases} r_i + A_{0i} (r_i^P + S_i^M) - A_{0j} (S_j^M - r_j^P) - r_j = 0 \\ -\tau_i^T \cdot A_{ij} \cdot \tau_j = 0 \end{cases} \quad (26)$$

By creating a cam design algorithm with the use of MAPLE, there were generated cam profiles. These are represented in Fig. 11 and Fig. 12. For these, the following input data were considered: $r = 5$ millimeters – cam roller radius; $x_i = 107$ millimeters; $y_i = 0$ – coordinates of the rotation center of the cam; $l_2 = 61,6$ millimeters – cam follower length; φ_2 - rotation angle of the cam follower.

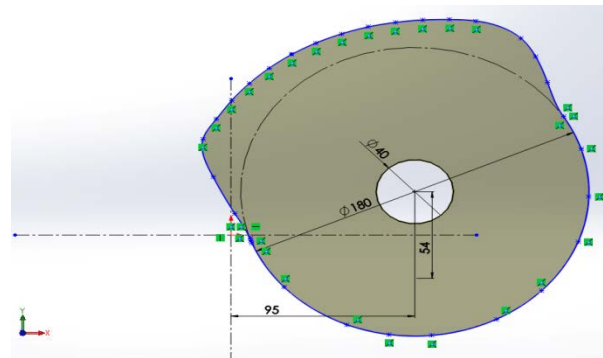


Fig. 11 Cam profile 3D model for knee actuation mechanism

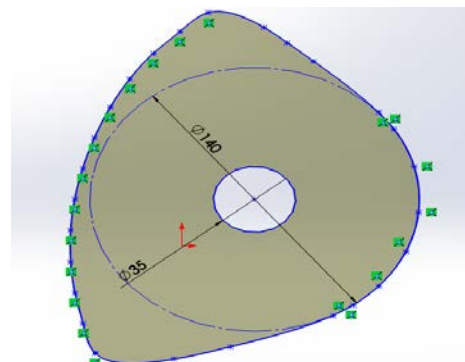


Fig. 12 Cam profile 3D model for ankle actuation mechanism

The second actuation system with linear electric actuators was created based on the first one and it is shown in Fig. 13. By considering the linkage notations from Fig. 8, it can be remarked that the linkage structure is almost the same.

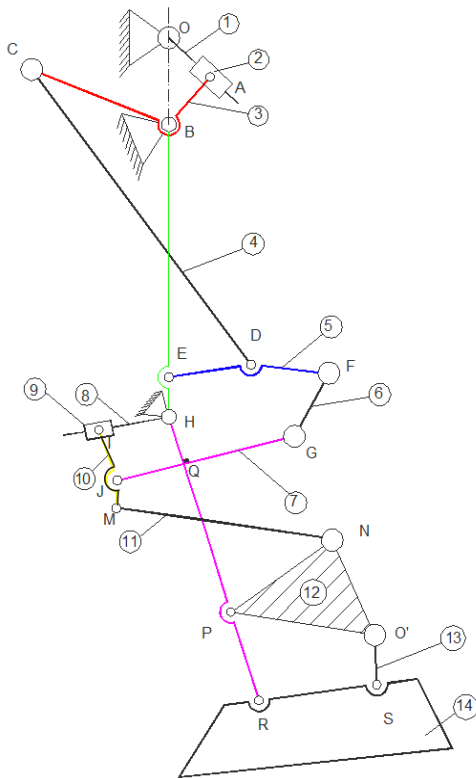


Fig. 13 Leg exoskeleton with linear actuators structural scheme

The input data for designing the cam mechanism were considered the ones resulted from an inverse kinematic analysis. For these the starting point was considered the cam mechanism geometry depending on the exoskeleton dimensional parameters according with anthropometric data and human lower limb motion laws obtained through experimental analysis carried with CONTEMPLAS Equipment.

A difference between the cam actuation mechanism and this one was given by the increase of the links number (14 links) and also there are two translational joints equivalent to the linear actuators (A, I joints), for knee and ankle equivalent joints.

In case of hip actuation joint, due to the mechanism configuration this will be a self actuated joint due to the linear actuator position namely A-joint. Based on the schemes from Fig. 8 and Fig. 13, virtual models of the proposed leg exoskeletons were designed and analyzed through numerical simulations with MSC Adams software in dynamic modes according with [21] and [22]. For the second actuation mechanism proposal, from a dynamic analysis it was obtained the force variation required for the linear electric actuators design. Thus the proposed mechanisms can be identified through virtual models which are shown in Fig. 14 and Fig. 15, where also the links and joints correspondence were kept according with the structural schemes.

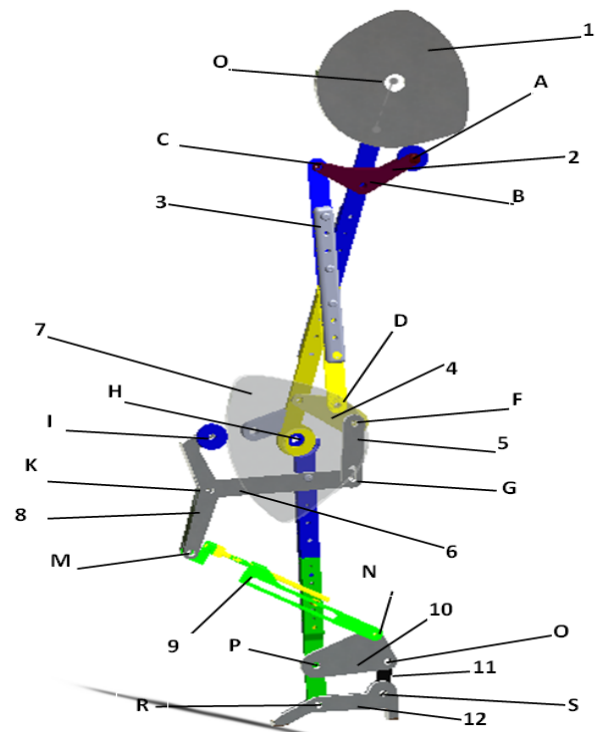


Fig. 14 Virtual model of the leg exoskeleton with cam mechanism

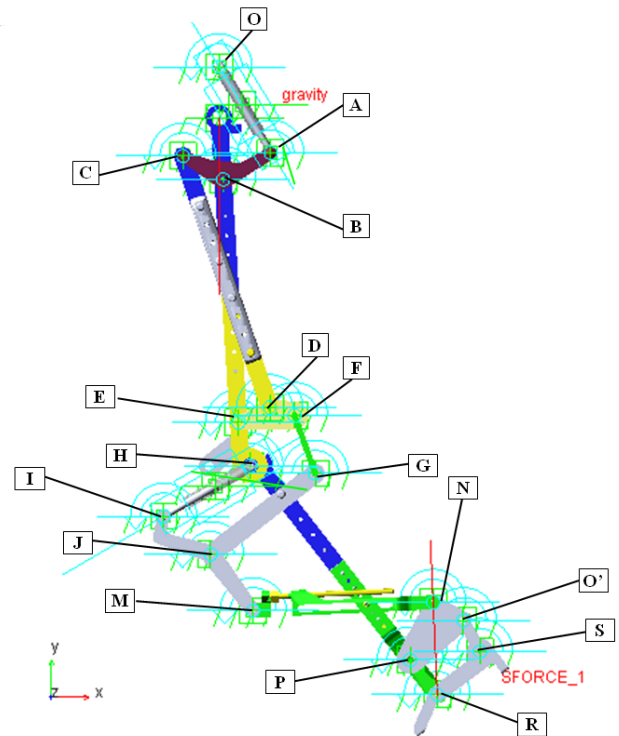


Fig. 15 Virtual model of the leg exoskeleton with linear actuators

The elaborated mathematical models were numerically simulated with the MSC Adams software aid for both actuation systems, by having as a kinematic reference element the variation law of the knee joint resulted from the experimental analyses. Thus it was created a kinematic simulation algorithm under the MSC Adams environment by having in sight the following steps: material property definition for each exoskeleton link, with proper inertial properties assignment;

kinematic joint definition, especially the ones for cam mechanism with proper angular velocities of the rotational actuators in such manner that these mechanisms should follow the command curve during gait simulation; numerical post processing and result evaluation. For both mechanical solutions structure, some design criteria were imposed based on important data considered from specialty literature reported in [25] and [26].

In real situation for using this prototype for human rehabilitation purposes, the proposed actuation mechanism should be for both human lower limbs and in this case the cam mechanisms for actuating the kinematic linkages for each human lower limb should work with an angular advance of 180 degrees, as it can be remarked in Fig. 16.

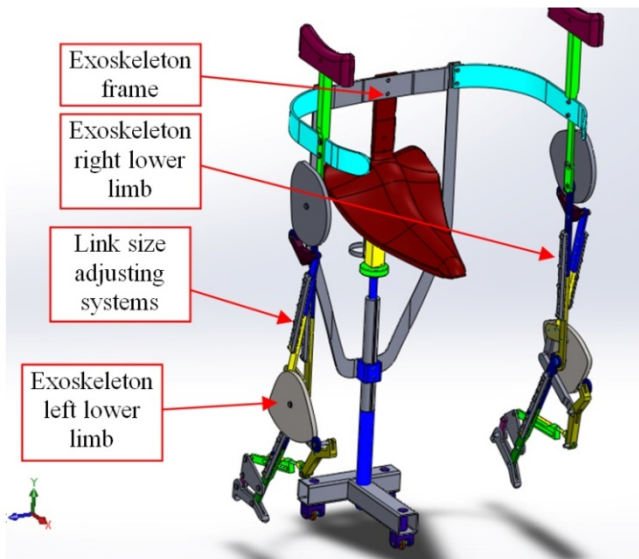


Fig. 16 Virtual model of the exoskeleton with cam mechanism actuation system for both lower limbs

Thus, in Fig. 16 it can be seen the entire exoskeleton virtual model with cam mechanism actuation. A detailed view of the cam disposal can be observed in Fig. 17 where proper cam mechanisms were defined under the MSC Adams environment.

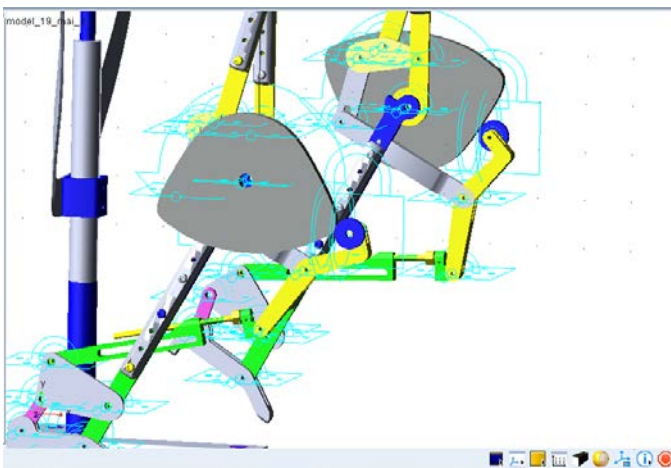


Fig. 17 Detailed view of the imported model in MSC Adams environment with cam mechanism joint definition in initial phase

In Fig. 17 it is represented a detailed view of the cams position for each human lower limb. Also a special frame was designed with a specific seat for placing the patient inside of the exoskeleton. This frame has a device for size variation with a mechanical transmission powered screw. The entire exoskeleton was designed in a modular form with adjustable size of each element in case of human lower limb femur and tibia parts and it can be adjusted for patient specific anthropometrical data.

Virtual simulations were performed for an equivalent time of **2.4 seconds** when a complete gait was achieved. Also the exoskeleton frame was fixed in space and the ground contact was not considered. For this case, important data were obtained after the results post processing and through these the proposed actuation mechanism was validated. Thus, in Fig. 18, Fig. 19, Fig. 20, Fig. 21 and Fig. 22 it can be remarked comparative results between both lower limbs for a complete gait.

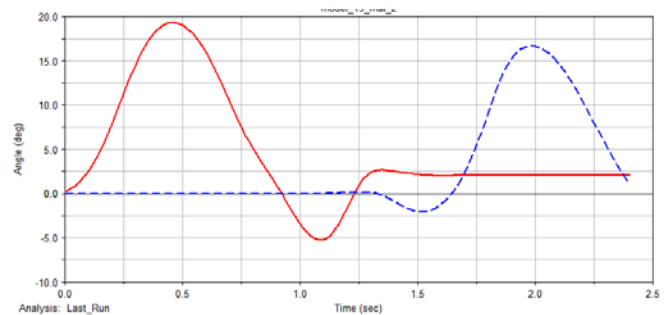


Fig. 18 Acquired motion law for exoskeleton knee joint (continuous line for right limb, dotted line for left limb) vs. time

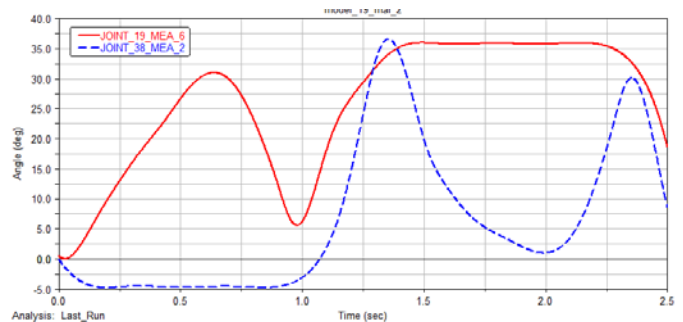


Fig. 19 Acquired motion law for exoskeleton ankle joint (continuous line for right limb, dotted line for left limb) vs. time

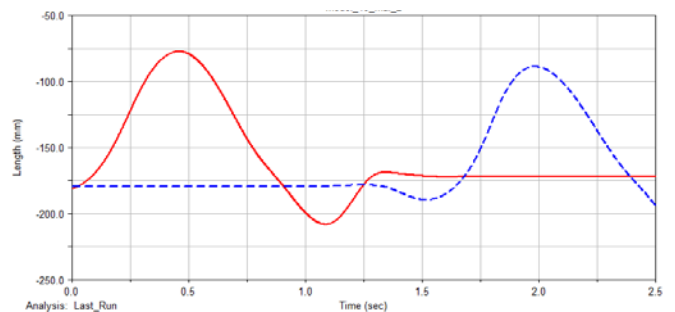


Fig. 20 X- component trajectory variation for point R (continuous line for right limb, dotted line for left limb) vs. time

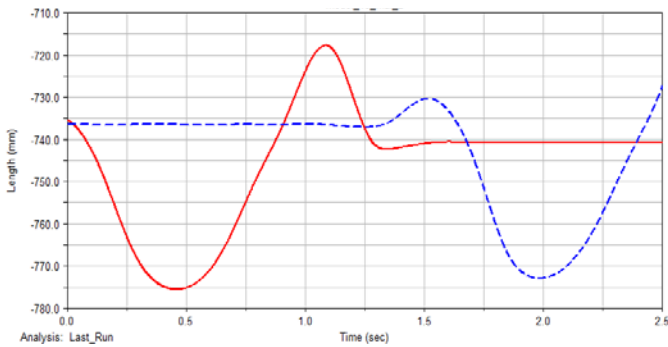


Fig. 21 Y- component trajectory variation for point R (continuous line for right limb, dotted line for left limb) vs. time

The angular amplitude variation in case of knee joints reaches a value of 19.75 degrees for right limb and 16.98 degrees for left limb. These values respect the variation laws for knee joint during walking in case of a healthy person, both it can be remarked a difference between them due to the missing patient payload.

Other comparative results can be remarked in case of ankle variation motion laws obtained through virtual simulations of the proposed mechanism in case of R joint, according with Fig. 8 for both exoskeleton limbs.

These results are represented by the translation displacements for specific markers attached on R joint which corresponds with ankle joint, for analyzing the leg extremity motion. In Fig. 19 it is shown the ankle joint motion law for both exoskeleton lower limbs virtual model where it can be remarked an angular amplitude between -4.75 to 36.23 degrees and also this corresponds with a ankle joint motion law for a healthy human subject in case of walking activity.

Other important results are represented by trajectory components on X and Y axis of the coordinate reference systems as it can be shown in Fig. 20 and Fig. 21. On these diagrams it can be observed that the feet rise with a maximum displacement of 50 millimeters and the half gait length for a single exoskeleton limb of 125 millimeters.

For a kinematic analysis of the ankle joint actuation mechanism, the reference system will be placed in H joint. Thus, it can be remarked that there were obtained similar results for R point displacement, which demonstrates that the cams were well designed, based on cam command curvature obtained through kinematic synthesis of the analyzed linkages.

By having in sight the obtained diagrams for R joint, which corresponds to ankle joint, it can be remarked that there is no difference between the motion amplitudes, due to the cam angular advance mounting of 180 degrees. Another aspect, which can be remarked in Fig. 17, is that in case of the right lower limb, the cam element is in a continuous contact with the cam follower command curve, meanwhile for the left lower limb the cam is in contact with the cam follower on the circular profile of the base circle. In this way it can be explained the cam advance position for left lower limb and between the curves for R joint, when the cam follower is situated on cam base circle.

IV. RECONFIGURABLE LEG EXOSKELETON PROTOTYPE ANALYSIS

By considering the virtual models validation through simulations, there were defined some technological parameters for choosing the proper actuators. These parameters are represented by torques for cam mechanism actuation and for the second actuation mechanism it was identified a technological force used on choosing proper linear actuators.

Thus, two prototypes were elaborated with the proposed actuation systems as it can be remarked in Fig 22 and Fig. 23.

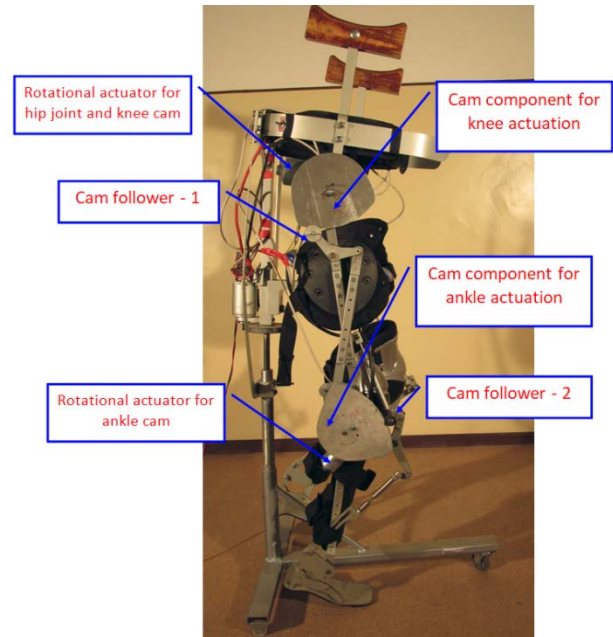


Fig. 22 Leg exoskeleton prototype with cam actuation mechanisms and rotational electric motors

For the first leg exoskeleton type there were chosen DC Motors of 24V and a nominal torque of 40Nm. In case of the second leg exoskeleton type there were used two linear electric actuators, respectively for knee actuation joint a SMC LEY- 32 Series linear electric actuator with a technological force of 707 Newton and a motion linear displacement of 200 millimeters. In case of the ankle joint, the adopted linear actuator was a Firgelli 856 type with a technological developing force of 70 Newton and a motion linear displacement of 125 millimeters.

These actuators used for second solution where chosen by considering the payload of each human lower limb. Thus, on the hip joint the load is in some gait phases equal with the human subject. As regarding the ankle joint actuator namely Firgelli 856, this was chosen as a small actuator due to the accomplished task, respectively it has to lift off the foot fingers when the foot is in the air.

The leg exoskeleton mechanical structure for both solutions was manufactured from aluminum alloys (N AW 2017 ALCU4MGSI type), and the command&control system was designed with an ARDUINO Mega 2560 Board equipped with a microcontroller ST7 type from SGS-THOMSON. The mechanical structure was also designed with additional devices for links dimensional adjustment in order to adapt the leg exoskeleton to any human subject with a height between 1.50 meters and 1.85 meters.

The ARDUINO board was used only for linear actuators motions and in case of actuation mechanism based on cams, it was necessary to add a microcontroller for controlling the rotational DC Motors.

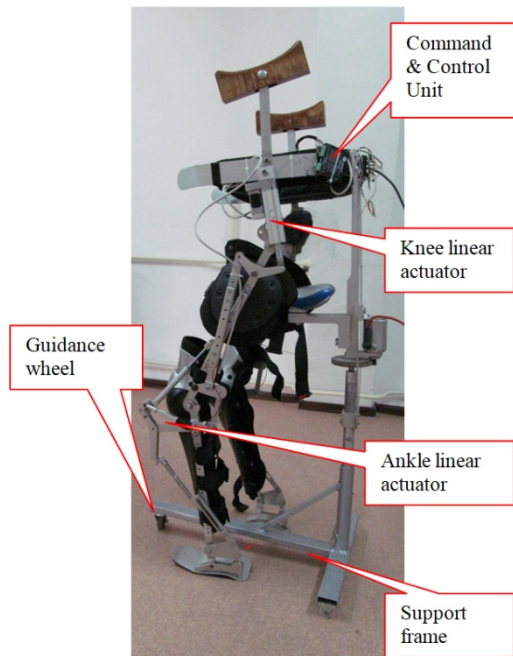


Fig. 23 Leg exoskeleton with linear actuators prototype

Between these two electronic components an electronic switch was placed in order to activate/deactivate the microcontroller by changing the actuation mechanisms. All linear actuators power supply was assured through one 24Volts DC accumulator. A command&control unit hardware was placed on the back of the exoskeleton frame as it can be observed in Fig. 23, and a detailed view of the hardware unit is shown in Fig. 24. Also the exoskeleton was equipped with proximity sensors in order to identify the limits between the exoskeleton links.

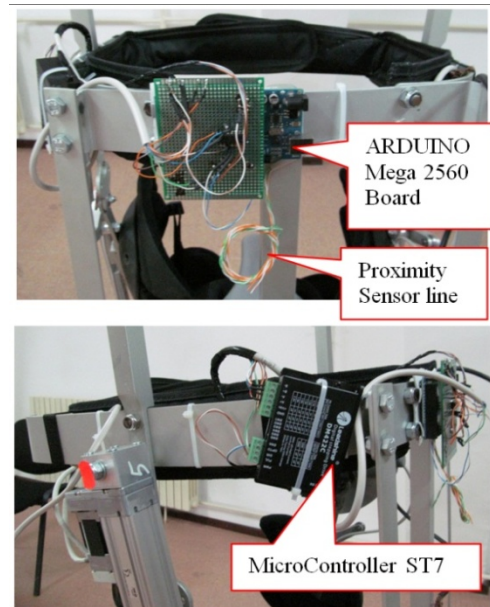


Fig. 24 Exoskeleton hardware unit for command and control

The proximity sensors role is to maintain the exoskeleton orientation, which in this case this is assured by placing and additional support which carries the whole exoskeleton structure and the patient on three wheels and one of these can be rotated free around an angle of 360 degrees. This can be remarked in Fig. 24.

For exoskeleton functionality principle, the angular variation of the human lower limb main joints identified in Fig. 4, Fig. 5 and Fig. 6, there were identified the maximum and minimum values corresponding to each gait phase. These represents the programming variables used as input parameter when a proper code protocol was written for Arduino Board. A part of it is shown in Fig. 25. This is a simple programming algorithm and it was loaded into Arduino storage memory. A diagram, which represents the Arduino program architecture, is shown in Fig. 26.

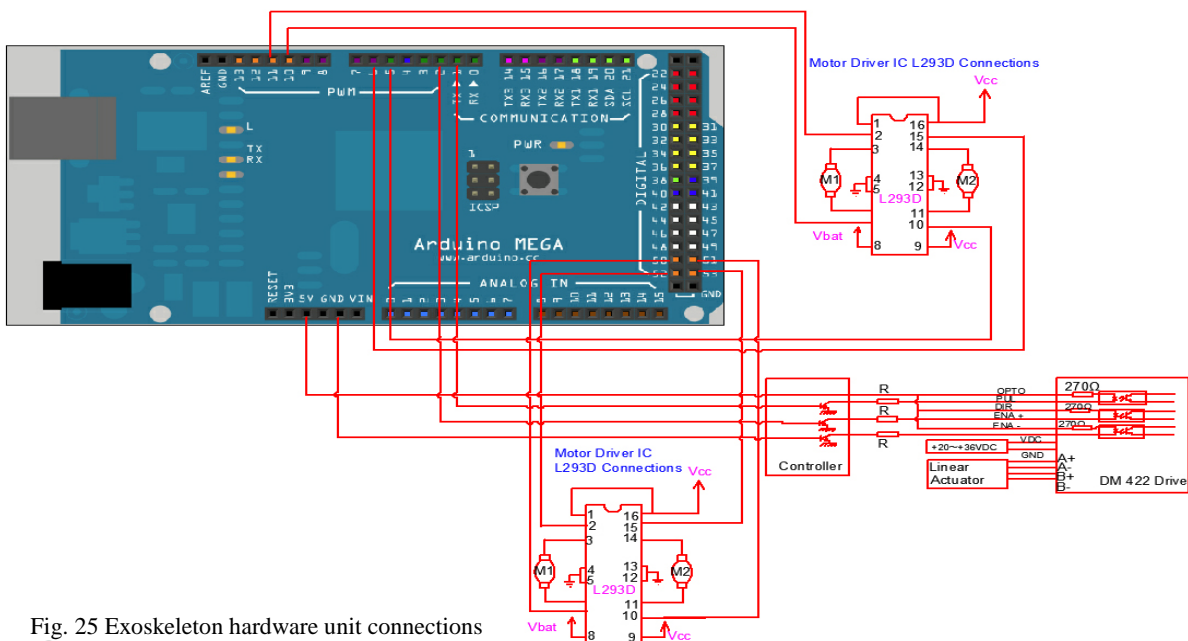


Fig. 25 Exoskeleton hardware unit connections

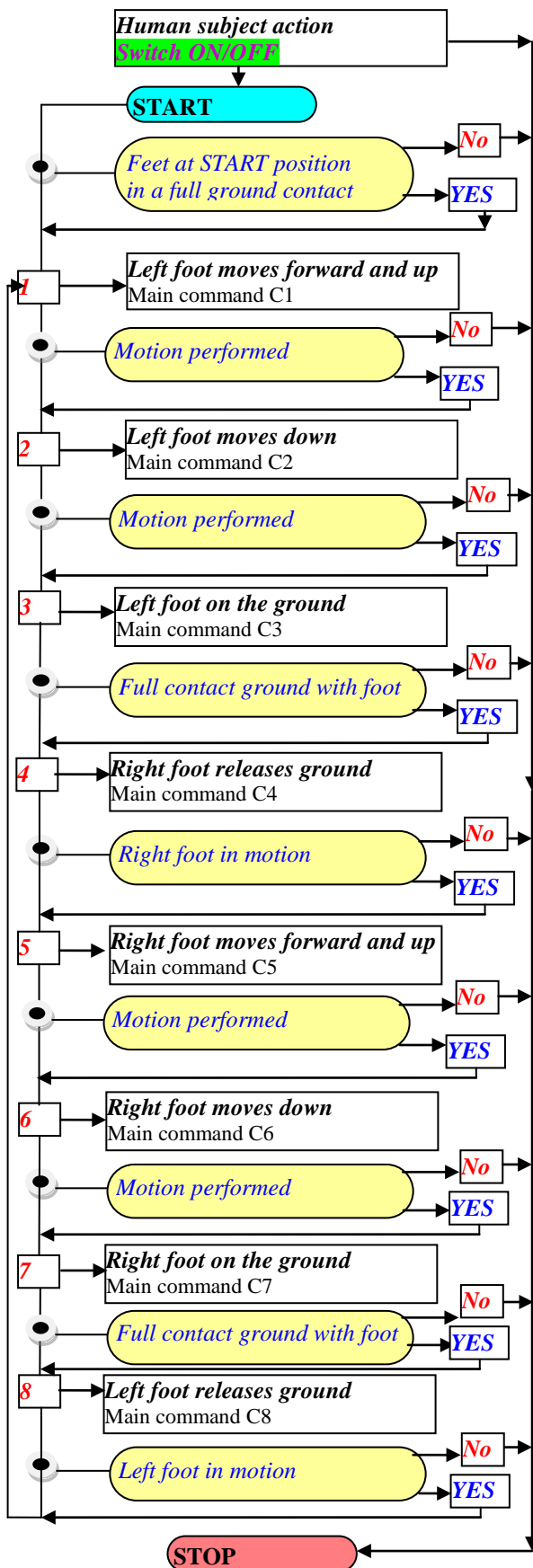


Fig. 26 Algorithm for exoskeleton command&control

In diagram from Fig. 26 it can be identified a variable and function series which can be summarized in main commands as it follows: C1-[Do: L_1 (0 to 100) and L_2 (-10 to 56); while $R_1=R_2$ =delay of 100]; C2-[Do: L_1 (100 to 5) and L_2 (56 to 5); while $R_1=R_2$ =delay of 95]; C3-[Do: L_1 (5 to 0) and L_2 (5 to 0); while R_1 (0 to -50) R_2 (0 to -52)]; C4-[Do: $L_1=L_2$ =delay of 50; while R_1 (-50 to 0) R_2 (-52 to -10)]; C5-[Do: $L_1=L_2$ =delay of 100; while R_1 (0 to 100) R_2 (-10 to 56)]; C6-[Do: $L_1=L_2$ =delay of 95; while R_1 (100 to 5) R_2 (56 to 5)]; C7-[Do: L_1 (0 to -50) and L_2 (0 to 52); while R_1 (5 to 0) R_2 (5 to 0)]; C8-[Do: L_1 (-50 to 0) and L_2 (-52 to -10); while $R_1 =R_2$ = delay of 50].

Where: L_1 – left knee linear actuator; L_2 – left ankle linear actuator; R_1 – right knee linear actuator; R_2 – right ankle linear actuator.

By considering that the exoskeleton is applied on human subjects, there were taken automatic safety decisions represented by two modes namely: each exoskeleton joint has a mechanical limitation; the patient has an easy access to a switch for power of the exoskeleton in case of emergency breakdown.

Thus, both leg exoskeleton types were experimentally tested and the obtained results were compared with the ones obtained on database with the aid of CONTEMPLAS Equipment. Also some experimental tests were performed on human subjects with locomotion problems at the level of left lower limb. The outputs for these tests can be remarked as a comparison results in Fig. 27, Fig. 28 and Fig. 29. These results were filtered with an algorithm encapsulated on CONTEMPLAS – Templo Motion software.

The experimental analysis was performed in the same conditions as the ones applied on healthy subjects. Through this both solutions can be validated.

In case of diagram from Fig. 27, it can be observed that the angular variation of both solutions is not so smooth for these particular cases like in case of an analyzed healthy subject.

Another remark is that the angular variations are in the range limit mentioned for the hip variations upper and lower limits as it is shown in Fig. 4. Moreover it can be observed a smooth curve for the solution with linear actuators, but the value range is smaller than in the second case namely cam mechanism.

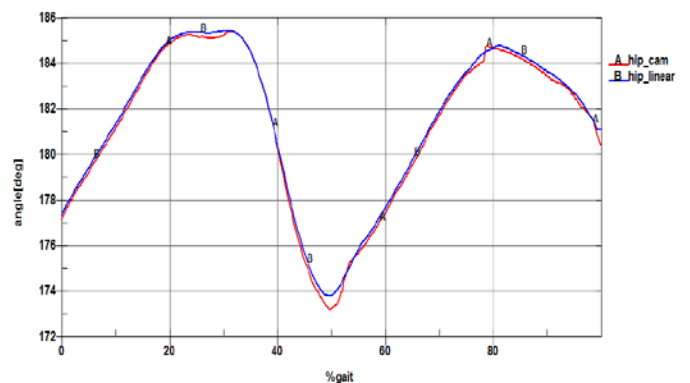


Fig. 27 Measured limits of the hip joint angle as function of % gait phase for the reconfigurable exoskeleton

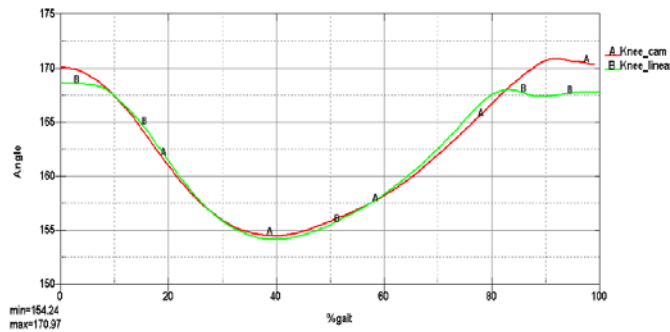


Fig. 28 Measured limits of the knee joint angle as function of % gait phase for the reconfigurable exoskeleton

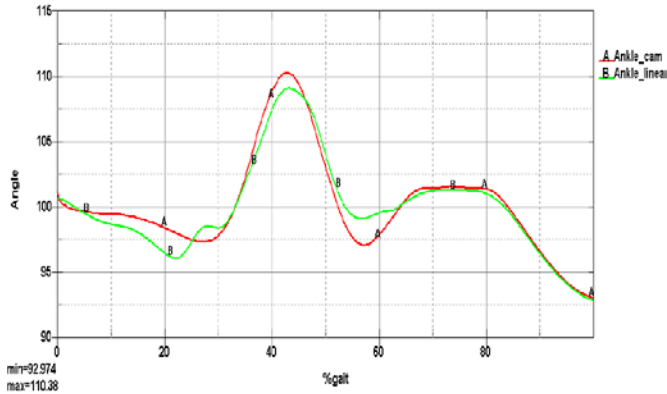


Fig. 29 Measured limits of the ankle joint angle as function of % gait phase for the reconfigurable exoskeleton

For the knee joint comparison analysis, the range limit values are appropriate with the ones developed by a healthy subject in case of linear electric actuators solution. Also it can be remarked a small delay due to some clearances between links.

For the analyzed ankle joints, the obtained values are appropriate for both proposed solutions. For cam mechanism solution, the range is higher than the other with linear actuators solution. Also in Fig. 29 it can be observed that the obtained curve for linear actuator is not smooth and also can be remarked some small gaps due to the clearances between the ankle actuation mechanism links.

By considering the outputs after this experimental analysis it can be observed that the functionality of the linear actuators have a small deviance due to the precise motion control input data.

Other remark is the one that the obtained angular variations results are in the same motion range with the ones of healthy humans which means that both actuation system solutions are validated and meet the physician requirements.

V. CONCLUSION

A conceptual design is presented for a reconfigurable leg exoskeleton used in human walking rehabilitation.

By referring to human walking characteristics a leg exoskeleton mechanism has been conceived with as kinematic structure whose mechanical design can be used for two

rehabilitation purposes as an exoskeleton wearable by patients.

The proposed leg mechanism has been identified with a process of adjusting a linkage based on two actuation mechanisms, namely cam mechanisms and linear electric actuators system.

A database was created in order to identify of human joints upper and lower limit.

There were designed and numerically simulated with MSC Adams software both exoskeleton proposed constructive solutions in a 3D mode when the actuation will be performed with cam mechanisms or linear electric actuators.

Based on the obtained analyses a command and control unit was designed for adapting the general mechatronic system at the human locomotion rehabilitation imposed requirements.

A prototype was elaborated and analyzed with capabilities for motion of hip, knee and ankle. In particular, the knee and ankle motions are obtained by proper cam mechanisms for persons with stroke or neuromotor disorders. Also these mechanisms can be replaced with linear electric actuators and the modified leg exoskeleton can be used for persons which follow temporal walking recovery programs after minor locomotion injuries.

The obtained prototype was validated through a comparison experimental analysis and both actuation mechanisms can be successfully used on human locomotion purposes on the same exoskeleton mechanical structure.

The reconfigurable exoskeleton is characterized by a flexible interface which can be easy adapted to any anthropometric data of the analyzed human subjects.

ACKNOWLEDGMENT

This work was supported by a grant of the Romanian National Authority for Scientific Research and Innovation, CNCS/CCCDI -UEFISCDI, project number PN-III-P2-2.1-PED-2016-0934, within PNCDI III.

REFERENCES

- [1] A. Esquenazi, M. Talaty, A. Jayaraman, *Powered exoskeletons for walking assistance in persons with central nervous system injuries: a narrative review*, PM & R9. 2017. pp. 46–62.
- [2] D.R. Louie, J.J. Eng, "Powered robotic exoskeletons in post-stroke rehabilitation of gait: a scoping review", *J. Neuroeng. Rehabil.* Vol. 13/53. 2016.
- [3] M. Bortole, A. Venkatakrishnan, F. Zhu, et. al., *The H2 robotic exoskeleton for gait rehabilitation after stroke: early findings from a clinical study*. Journal of NeuroEngineering and Rehabilitation. Vol. 12:54. 2015. pp. 1-14.
- [4] S. Federici, F. Meloni, M. Bracalenti, M.L. De Filippis, *The effectiveness of powered, active lower limb exoskeletons in neurorehabilitation: a systematic review*. Journal of Neuro-Rehabilitation. Vol. 37. 2015. pp. 321–340.
- [5] Pons JL. *Wearable robots: biomechatronic exoskeletons*. Chichester, UK: John Wiley & Sons, Ltd, 2008.
- [6] Banala SK, Agrawal SK and Scholz JP., "Active leg exoskeleton (ALEX) for gait rehabilitation of motor-impaired patients". In *IEEE 10th international conference on rehabilitation robotics* (eds B Driessen, JL Herder, GJ Gelderblom), 13–15 June 2007, Noordwijk, Netherlands, pp. 401–407. IEEE. DOI: 10.1109/ICORR.2007.4428456
- [7] Sergi F. *Biomechatronic design of wearable and operational robots for rehabilitation and assistive applications terza linea*. Roma, Italy: Universita` Campus Bio-Medico di Roma School of Engineering, 2011.

- [8] Dumitru N., A. Didu, C. Copilusi, *Mechatronic system for locomotion rehabilitation*. Advances in Engineering and Management. ISSN 2537-4443. 2016. pp. 53-54.
- [9] Dumitru N., Copilusi C., Geonea I., et. al., *Dynamic Analysis of an Exoskeleton New Ankle Joint Mechanism*. In: Flores P., Viadero F. (eds) New Trends in Mechanism and Machine Science. Mechanisms and Machine Science, vol 24. Springer. 2015
- [10] Jonas Beil, Gernot Perner and Tamim Asfour, "Design and Control of the Lower Limb Exoskeleton KIT-EXO-1". *Proceedings of IEEE International Conference on Rehabilitation Robotics (ICORR)*. 2015. pp. 119-124.
- [11] Yu S, Han C and Cho I., *Design considerations of a lower limb exoskeleton system to assist walking and load-carrying of infantry soldiers*. Appl Bion Biomech 2014; 11(3): 119–134.
- [12] Lopez R, Aguilar H, Salazar S, et al., *Modelado y Control de un Exoesqueleto para la Rehabilitación de Extremidad Inferior con dos grados de libertad*. Rev Iberoam Automatica e Informatica Ind RIAI 2014; 11(3). pp. 304–314.
- [13] Galle S, Malcolm P, Derave W, et al., *Adaptation to walking with an exoskeleton that assists ankle extension*. Gait Posture. 2013; 38(3). pp. 495–499.
- [14] Strausser KA, Zoss AB, Swift TA, et al., *Mobile exoskeleton for spinal cord injury: development and testing*. In Proceedings of the ASME 2011 dynamic systems and control conference, Arlington, VA, USA, 31 October–2 November 2011, pp. 419–425. DOI: 10.1115/DSCC2011-6042
- [15] Geonea, I. D., Margine, A., Dumitru, N., Copilusi, C., *Design and simulation of a mechanism for human leg motion assistance*. In Advanced Materials Research Vol. 1036, pp. 811-816. 2014.
- [16] Ghobrial GM and Wang MY., *The next generation of powered exoskeleton use in spinal cord injury*. Neurosurg Focus 2017; 42(5): E16.
- [17] S.H.You, *Concurrent Validity and Test-Retest Reliability of the Novel Walkbot-K System*. J. Mech. Med. Biol. 16. 2016.
- [18] CONTEMPLAS Motion Analysis Equipment *User Manual* Accessed in 2016.
- [19] N.L.W. Keijsers, N.M. Stolwijk, G.J. Renzenbrink, J. Duysens, *Prediction of walking speed using single stance force or pressure measurements in healthy subjects*. Journal of Gait & Posture. Vol. 43. pp. 93–95. 2016
- [20] Pirker, W., Katzenschlager, R., *Gait disorders in adults and the elderly: A clinical guide*. Wiener klinische Wochenschrift. 2016. 129.10.1007/s00508-016-1096-4.
- [21] MSC Adams software *User Manual*. Accessed in 2017.
- [22] Steinicke F, Visell Y, Campos J, et al., *Human walking in virtual environments*. New York, NY, USA: Springer, 2013.
- [23] Duffy J., *Statics and kinematics with applications to robotics*. New York, NY, USA: Cambridge University Press, 1996, pp. 173.
- [24] Chiacchio P, Chiaverini S, Sciavicco L, et al., *Closed-loop inverse kinematics schemes for constrained redundant manipulators with task space augmentation and task priority strategy*. Int J Rob Res 1991; 10: 410–425.
- [25] Robert L.Norton. *Design of machinery*. McGraw-Hill,2008.
- [26] Charles E.Wilson, J.Peter Sadler. *Kinematics and dynamic of machinery*. HarperCollins College Publishers,1993